ISSN 2176-5480

22nd International Congress of Mechanical Engineering (COBEM 2013)
November 3-7, 2013, Ribeirão Preto, SP, Brazil
Copyright © 2013 by ABCM

DYNAMIC ANALYSIS AND STABILITY CONDITIONS IN ROTATING SYSTEMS WITH TILTING PAD JOURNAL BEARING

Antonio Carlos Carneiro, acarneiro@fem.unicamp.br
Gregory Bregion Daniel, gbdaniel@fem.unicamp.br
Katia Lucchesi Cavalca, katia@fem.unicamp.br
Laboratory of Rotating Machinery – Faculty of Mechanical Engineering – Postal Box 6122
University of Campinas - UNICAMP
13083-970, Campinas, SP, Brazil

Abstract. *The dynamic analysis of rotating machines involves an elevated degree of complexity. In the analysis, the dynamic behavior of the rotor should be analyzed considering its interaction with other components of the same system. In a rotor-bearing-foundation system, the vibration applied by the rotor is transferred through the bearings to the supporting structure, in which interacts with the bearings retransmitting the vibration to the rotor. In this way, the bearings have an important role in this system, because this component is responsible to transmit forces between the rotor and the support structure. For this reason, the dynamic behavior of the bearings must be considered in the mathematical model of the complete system. This work aims to evaluate the tilting pad bearings' stability condition, because the dynamics characteristics of these bearings allow its application on machines with high rotation speed and low load, which can lead to fluid-induced instability in journal bearings with fixed geometry. In face of that, the stiffness and damping coefficients of a tilting pad journal bearing are determined and applied in the dynamic analysis of rotating systems supported by these components to evaluate the stability condition of the complete system. The first analysis is accomplished to a cylindrical journal bearing with similar dimensions of the tilting-pad bearing. The second analysis uses the reduced equivalent coefficients, in which a reduction of the dynamic model of the bearing is accomplished in order to obtain equivalent coefficients represented only by the translational coordinates. In both approaches, the stability analysis aims to understand and evaluate the sensitivity degree of the design parameters involved in this phenomena.*

Keywords: *tilting-pad journal bearings, rotordynamics, hydrodynamic lubrication, stability*

1. INTRODUCTION

The dynamic analysis of rotating machinery involves an elevated number of variables, which require a careful treatment and great attention, in order to reach high accuracy and representative solution of the real behavior of the machine. This is more evident when the analysis has to represent the interaction with others components and elements, for instance, a rotor-bearing system. The bearings play an important role in the dynamic analysis of rotating systems, in which they can be represented by dynamic coefficients that must be accurately determined and carefully added to the rotor model.

There are numerous kinds of bearings, but one of the most commonly used in rotating machines is the hydrodynamic, due its high life cycle and load capacity. Among the lubricated bearings, the tilting-pad journal bearings stands out, because it can be used in critical operation conditions, i.e. high rotational speed and low load, without to become susceptible to fluid-induced instabilities (oil-whirl and oil-whip). Prior to the development of tilting-pads, due to critical operational conditions, design engineers used to focus on geometry changes applied to cylindrical bearings, resulting in multilobe and elliptical designs. Still, even those bearings configurations are likely to present the whirl-whip phenomenon, which partially explains the development of tilting-pad journal bearings.

The development of the theory for hydrodynamic bearings started with Reynolds (1886), who first created the mathematical model for the hydrodynamic lubrication. The Reynolds' Equation relates the pressure field caused by two surfaces separated by a fluid film. Along with the analytical solution for long bearings, as proposed by Sommerfeld (1904), these two events initiated the theoretical development of the hydrodynamic bearings. In the years that succeeded, it can be highlighted the works of Stodola (1925) and Hummel (1926), that proposed the equivalent stiffness and damping coefficients in order to represent the effects caused by the fluid film.

Another important observation was made by Newkirk and Taylor (1925), who published that the vibration on a hydrodynamic bearing could not be due by unbalancing forces or internal friction, but induced by the fluid itself. These fluid-induced instabilities were, and still are, widely studied to predict the behavior of the shaft, to improve the machine's and bearings' designs, and to prevent serious operational failures. Presently, it is well established that oil-whirl is related to the lubricant fluid characteristics, and oil-whip is relative to the system's natural frequencies.

Theretofore, most of the bearings used in the real applications were short bearing and there was not an analytical solution to describe the behavior of this kind of bearing. Thus, Ocvirk (1952) accomplished a highlighted work in which presented a solution to the problem for a short bearing.

ISSN 2176-5480

The development of computational systems had great influence on the evolution of bearings' theory. From that period, Pinkus (1956, 1958, 1959) used the finite differences method to model the pressure inside a bearing, resulting on great advances on the research's field.

The tilting-pad journal bearings only became relevant in the industry when the cylindrical bearings were not able to operate safely with the growing needs of rotational speeds. The groundbreaking work on the subject was published by Lund (1964), where a methodology was presented to obtain the dynamic coefficients of a tilting-pad journal bearing. It's important to highlight that Lund's method compress the influence of the pads' tilting motion into shaft translation degrees of freedom, by assuming that the frequency of the pads' motions are synchronous with the shaft rotation speed. Lund's work opened a new path in bearings' research, allowing a large expansion in the usage of tilting-pad journal bearings.

Another advance was made by Allaire, *et al.* (1981), which were able to obtain coefficients that explicitly represented the tilt motion, through a pad-perturbation method, resulting in full dynamic coefficients. Afterwards, those coefficients could be synchronously reduced, if necessary, in order to obtain equivalent coefficients related only with the translational degrees of freedom. Through the 1980's and 1990's more effects were investigated in analyses made by several authors, such as pivot elasticity, pad deformation, oil temperature; all aiming to a more precise representation of the bearing and system behavior.

This work goal is to compare the stability margin of a Laval rotor supported by two different kinds of bearings: a cylindrical bearing, and a 5-pad tilting-pad journal bearing, in order to evaluate the stability region of both rotors configurations.

2. METHODOLOGY

The dynamic analysis of a rotating system has to join different kinds of analyses, such as the determination of damping and stiffness coefficients or modeling of the shaft. Moreover, one must know that these distinct analyses depend on each other; for instance, to obtain the coefficients it's necessary to know the static load that the shaft exerts on the bearings.

An analysis starts with the obtaining of the static load of the bearing. After that, bearing's stiffness and damping coefficients were obtained and finally the finite element modeling of the shaft is made. The shaft's global matrixes (Mass, Damping, Stiffness, and Gyroscopic Effect) are assembled, altogether with the bearings' and discs' representations being added into their corresponding nodes' positions, in the matrixes.

Finally, there are many ways to observe and analyze the system's dynamic behavior: applying the concept of mechanical impedance into the equation of motion, one can obtain the frequency response of the system and, therefore, to verify the amplitude and phase of the shaft's circular motion. Also, the system's equation of motion can be written in state-space representation, which allows the integration of the equation in time domain; in this way, one can observe the orbits of the shaft inside the bearing. The state-space representation also permits the obtaining of the Campbell's diagram and the free vibrational modes, through the solution of an eigenvalue and eigenvector problem.

2.1 Determination of Dynamic Coefficients

The determination of the dynamic coefficients of a bearing is a procedure that has to combine knowledge from fluid mechanics, when evaluating the Reynolds' Equation, and solid mechanics, when using the concept of equivalent dynamic coefficients.

The stiffness and damping coefficients of a journal bearing are obtained through the solution of the Reynolds' Equation, shown in Eq. (1). Equation (1) relates the pressure field, which arises from the relative motion inside the bearing, with the bearing's internal oil-film thickness and velocity of the relative motion. Therefore, it's possible to determine the pressure field and, hence, the hydrodynamic forces and dynamic coefficients. However, Reynolds's Equation has limited analytical solutions available; so its solution tends to be obtained through mathematical methods, such as the finite volume method.

$$-\left(\frac{h}{-}-\right)+-\left(\frac{h}{-}-\right)= \qquad \frac{h}{-}+ \qquad \frac{h}{t} \tag{1}$$

Where *P(x,z)* is the pressure distribution in the oil film, *x* and *z* are the rectangular coordinates,   is the absolute viscosity, *R* is the radius of the shaft, *h* is the thickness of the oil film,   is the rotational speed and *t* is the time.

The solution starts with the search for the equilibrium position of the shaft inside the bearing through a Newton-Raphson method, for each rotational speed. Afterwards, a small perturbation around the equilibrium is applied separately to every degree of freedom, which induces a perturbed pressure profile; then the pressure can be integrated to give the perturbed forces, as described by Lund (1964, 1979, and 1987). The perturbed forces can be represented through a first order Taylor series expansion, as showed in Eq. (2).

ISSN 2176-5480

$$
\begin{aligned}
F_x &= K_{xx}\Delta x + K_{xy}\Delta y + C_{xx}\Delta\dot{x} + C_{xy}\Delta\dot{y} \\
F_y &= K_{yx}\Delta x + K_{yy}\Delta y + C_{yx}\Delta\dot{x} + C_{yy}\Delta\dot{y}
\end{aligned}
\tag{2}
$$

Equation (2) relates the perturbed forces, indicated by F_x and F_y, with the perturbations applied on each degree of freedom (Δx, Δy, $\Delta\dot{x}$, $\Delta\dot{y}$). Therefore, the coefficients can be evaluated as partial derivatives at the equilibrium position (Lund, 1987), as showed exemplified in Eq. (3). The remaining coefficients are similarly obtained.

$$
K_{xy} = \left(\frac{\partial F_x}{\partial y}\right)_0 \qquad C_{xy} = \left(\frac{\partial F_x}{\partial \dot{y}}\right)_0 \tag{3}
$$

This paper compares the dynamic behavior of a rotating shaft, under the same operational conditions, but firstly supported by cylindrical bearings and secondly by tilting-pad journal bearings. It must be highlighted that in the cylindrical case, the perturbations are applied in the displacement and velocity of the shaft, exactly as shown in Eqs. (2) and (3). This procedure results in four stiffness and four damping coefficients (Machado, 2009).

However, in the tilting-pad journal bearing, in addition to the perturbations applied to the shaft's translational degrees of freedom, the perturbations in displacement and velocity must be done to every pad's tilting degree of freedom (α_1, α_2 to α_N, in a tilting-pad bearing with N pads). The presence of extra degrees of freedom results in more coefficients than the eight previously mentioned; in a journal bearing with 5 pads, for instance, 18 coefficients are obtained (Daniel, 2012).

To overcome this excess of coefficients, it is usual to reduce the equivalents coefficients related to pads' motions, leading to the coefficients with translational coordinates only, giving, like the cylindrical ones, eight coefficients. However, the coefficient's reduction procedure depends on the vibration frequency that must be assumed to the pads' vibration. In this paper, the frequency of the pad's motion is assumed to be synchronized with the shaft rotational speed, giving "synchronously reduced" coefficients.

2.2 Finite Element Representation

The mathematical model of the shaft is obtained by the finite element method, which turn possible the representation of a continuum object into discrete elements. Regarding the rotordynamics, a discretization based on a two-node finite element is adequate to represent the shaft's dynamic behavior. The matrixes used in this work were presented in Nelson and McVaugh (1976) and Nelson (1980), where the Timoshenko's beam theory is employed, as implemented by Tuckmantel (2010). Each element's matrixes are combined together to form global matrixes, containing all the degrees of freedom of the shaft's model. These global mass (*[M]*), stiffness (*[K]*), damping (*[C]*), and gyroscopic (*[G]*) matrixes are used in the equation of motion of the rotating system, as showed by Eq. (4), where the vector *{F}* contains the external forces and Ω is the shaft's rotational speed.

$$
[M]\{\ddot{u}\} + ([C] - \Omega[G])\{\dot{u}\} + [K]\{u\} = \{F\} \tag{4}
$$

The damping matrix, which represents the structural damping of the rotor, is considered proportional with the mass and stiffness matrixes, as indicated by Eq. (5).

$$
[C] = \alpha[M] + \beta[K] \tag{5}
$$

In this work, the damping matrix is considered to be proportional only with the stiffness matrix; hence, $\beta = 0.0002$.

After the assembly of the global shaft's matrixes, the shaft's external elements, such as rigid discs and the bearings, must be added on their corresponding nodes. The disc presents effects that must be added into the mass and gyroscopic effect matrixes; the bearings have stiffness and damping terms, as described in section 2.1.

2.3 Dynamic Analyses

The dynamic analyses of a rotating system have to observe several effects and phenomena, resulting from the shaft's motion, in order to correctly characterize the rotor behavior. In particular, there are some interactions that are only detected through studying the free vibration of the system, which is the homogeneous solution of the equation of motion. For this reason, it is possible to sort the different analyses into two types: the free response, or free vibration of the system, and the forced response, or vibration, of the system (Mendes, 2011).

2.3.1 Free Response

The free response analysis is useful to observe and estimate the natural frequencies of the system, and the free vibrational modes. This analysis is accomplished by rewriting Eq. (4) in a state-space form, as showed by Eq. (6). Since is a free response analysis, only the system's dynamic matrix, defined by Eq. (7), is accounted in the solution. Then, an eigenvalue and eigenvector problem is applied to the dynamic matrix to determine the natural frequencies of the system.

$$\begin{Bmatrix} \{\dot{\ }\} \\ \{\ddot{\ }\} \end{Bmatrix} = \begin{bmatrix} [\ ] & [\ ] \\ -[\ \ ]\ [\ ] & -[\ \ ]\ ([\ ] - \Omega[\ ]) \end{bmatrix} \begin{Bmatrix} \{\ \} \\ \{\dot{\ }\} \end{Bmatrix} + \begin{bmatrix} [\ ] & [\ ] \\ [\ ] & [\ \ ] \end{bmatrix} \begin{Bmatrix} \{\ \} \\ \{\ \ \} \end{Bmatrix} \tag{6}$$

$$[\ ] = \begin{bmatrix} [\ ] & [\ ] \\ -[\ \ ]\ [\ ] & -[\ \ ]\ ([\ ] - \Omega[\ ]) \end{bmatrix} \tag{7}$$

The resulting eigenvalues of the dynamic matrix are complex numbers, where the real part is related to the amplitude's decaying of the response, and the imaginary term gives the oscillatory feature of the response. The absolute value of the eigenvalue is the natural frequency of the system, and the damping ratio is the ratio between the real part of the eigenvalue and its modulus.

For the purpose of stability analysis, the real part must be observed: if the signal is negative, the function decays with time, giving a stable system. However, if the real part of the eigenvalue is positive, the function increases continuously with time, leading the system to instability condition.

With the solution of the eigenvalue problem, it is possible to elaborate the Campbell's diagram and observe the damping ratio of the system. The Campbell's diagram shows the variation of the natural frequencies of the system, versus the rotational speed of the shaft. The same can be done to the damping ratio. From the variation of the real portion of the eigenvalue, it is possible to observe the onset of instabilities, by observing the signal of the real part of the eigenvalue.

2.3.2 Forced Response

The forced response analysis is required for the dynamic analysis of a rotating system because a rotor is not perfectly balanced, having a residual mass located offset to the shaft's geometric center. This residual mass excites the rotor in the same frequency as its rotational speed, so, to observe the full system response, it is necessary to evaluate the particular solution of the equation of motion, given by the forced vibration of the shaft.

When the shaft is excited by a harmonic force, the system vibrates in the same frequency, but with different amplitude and phase. The frequency response function (FRF) provides a complex result, which can be graphically represented by module and phase, giving an overview of the system's response with the excitation frequency.

Since the force's and the response's frequencies are the same, the FRF can be evaluated using the mechanical impedance concept. The resulting equation, after manipulating Eq. (4), is shown in Eq. (8), where *{F}* is the vector of unbalancing forces, *{Q}* is the vector of amplitudes, and the mechanical impedance matrix is represented by Eq. (9).

$$\{\ \ \} = \left[-\Omega\ [\ \ ] + \ \Omega([\ \ ] - \Omega[\ \ ]) + [\ \ ]\right]\ \ \{\ \ \} \tag{8}$$

$$[\ \ ] = \left[-\Omega\ [\ \ ] + \ \Omega([\ \ ] - \Omega[\ \ ]) + [\ \ ]\right] \tag{9}$$

The second approach that is usually used is the evaluation of operational modes, or forced modes, of the shaft. The forced mode is a linear combination between all the natural modes existing within the shaft. This procedure allows the visualization of the displacement of the shaft and deformed shape of the mechanical system, under an external force.

3. RESULTS

The dynamic analysis is based on the Laval rotor, shown in Fig. 1.

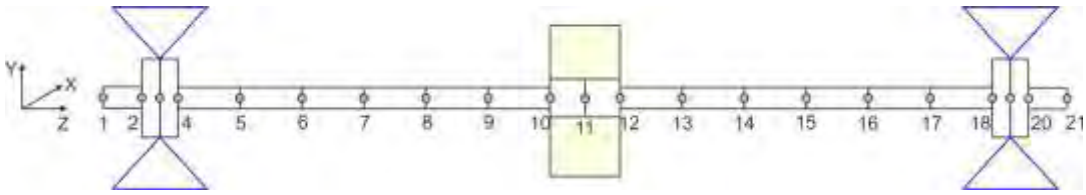

Figure 1. Schematic representation of the Laval rotor.

ISSN 2176-5480

Table 1 presents the dimensions considered for the rotor, where the disc's data has to account for the inner and outer diameters. Excitation is considered as unbalanced mass, and is positioned at node 11, on the disc, with a magnitude of 5.10^{-5} kg.m. The dynamic coefficients of the bearings are calculated from 600 RPM to 24000 RPM. The parameters for both bearings are in Tab. 2 and Tab. 3.

Table 1. Dimensions of the shaft

Element	**Element Type**	**Length (10^3 m)**	**Radius (10^3 m)**	**Element**	**Element Type**	**Length (10^3 m)**	**Radius (10^3 m)**
1	Beam	25.0	15.0	11	Disc	47.0	outer = 95.0 inner = 25.0
2	Beam	12.5	50.0	12	Beam	23.5	25.0
3	Beam	12.5	50.0	13	Beam	40.0	15.0
4	Beam	40.0	15.0	14	Beam	40.0	15.0
5	Beam	40.0	15.0	15	Beam	40.0	15.0
6	Beam	40.0	15.0	16	Beam	40.0	15.0
7	Beam	40.0	15.0	17	Beam	40.0	15.0
8	Beam	40.0	15.0	18	Beam	40.0	15.0
9	Beam	40.0	15.0	19	Beam	12.5	50.0
10	Beam	23.5	25.0	20	Beam	12.5	50.0
				21	Beam	25.0	15.0

Table 2. Parameters for the cylindrical bearing

Diameter of the Shaft	0.050 m
Width of the Bearing	0.025 m
Radial Clearance	70 μm
Lubricant Viscosity	$5{,}01.10^{-2}$ Pa.s (ISO-VG 32)

Table 3. Parameters for the tilting-pad bearing

Diameter of the Shaft	0.050 m
Width of the Bearing	0.025 m
Radial Clearance	70 μm
Lubricant Viscosity	$5{,}01.10^{-2}$ Pa.s (ISO-VG 32)
Pad Radius	0.0254575 m
Pad Thickness	0.0135 m
Pad Angle	63.5 °
Angle Between Pads	8.5 °
Pre-Load	0.847
Load Characteristic	On Pad

There are two analyses being considered: in the first, the shaft is assembled with cylindrical bearings; and in the second, the same simulation is made with a 5-pad tilting-pad journal bearing.

For the cylindrical case, the Campbell's diagram and damping ratio graphic are shown in Fig. 2.

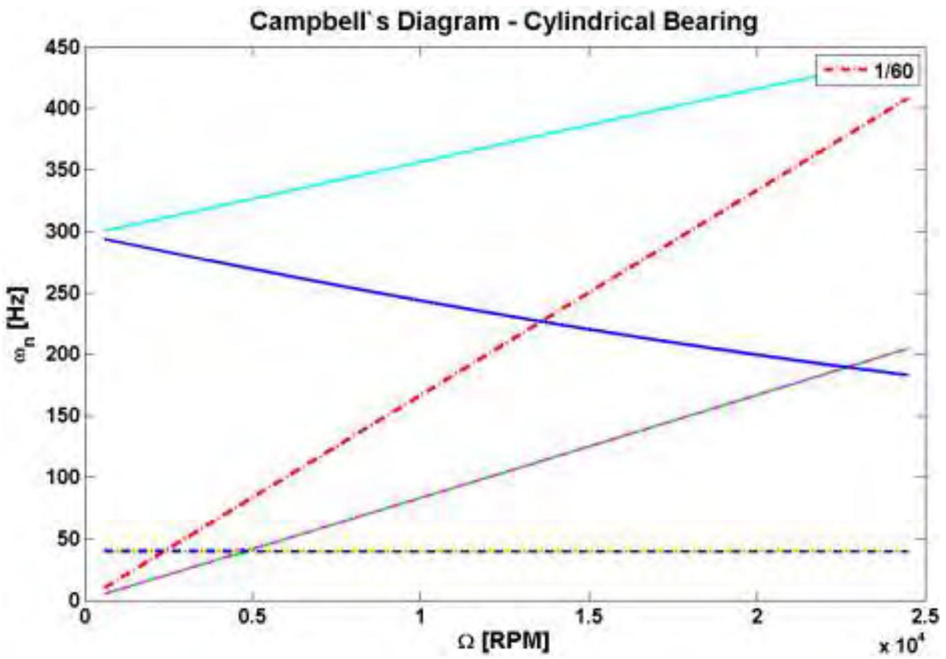

(a)

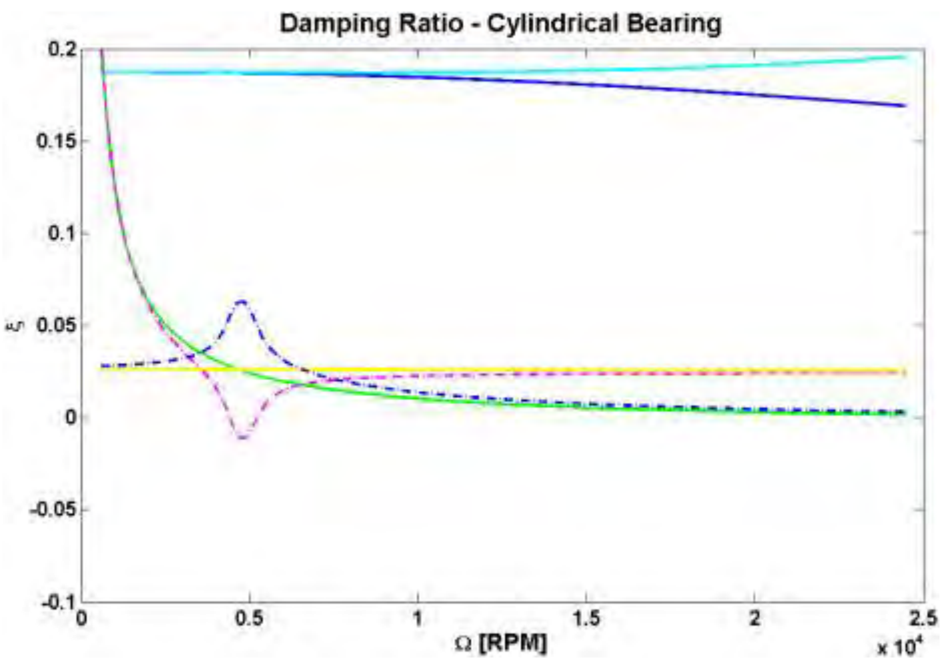

(b)

Figure 2. Free response for cylindrical bearing case: (a) Campbell's diagram; (b) Damping ratio.

Figure 2(a) shows the shaft's natural frequencies curves, the bearings' frequencies curve, and the dashed line is the rotation line (1/60 line), that indicates where the shaft rotational speed is equal to the natural frequencies. When the 1/60 line crosses one of the shaft's natural frequencies curves, the rotational speed is equal to a natural frequency. Thus, this crossing point is called critical speed, and in this case, it is close to 2400 RPM as in Fig. 2(a).

Another information is where the bearings' frequencies line crosses the shaft's frequencies. From the literature, this crossing point indicates the onset of fluid-induced instabilities (oil whip) and, for the cylindrical bearings case, is about to 2 times the shaft's first critical speed. This point is located on the rotational speed of 4800 RPM. For this reason, it is expected that instabilities occur, starting from this rotational speed.

Figure 2(b) shows the damping ratios related to the natural frequencies presented in Fig. 2(a). As discussed on the methodology, the damping ratio gives information about the threshold of instability, observing the point where the

ISSN 2176-5480

damping ratio becomes negative. As a result, it is possible to observe that around 4800 RPM the damping ratio is negative, indicating the imminence of an instable operational condition.

As expected, both graphics of Fig. 2 show consistent and coherent results, in agreement with the instable operation of the shaft observed around 4800 RPM.

Fig. 3 shows the orbits found through the response in time domain at a rotational speed of 4320 RPM, i.e. before the evaluated threshold of instability. A decreasing behavior for the orbits can be noticed over the time, for both Fig. 3(a) and (b), which indicates that the shaft have a stable operation in this rotational speed.

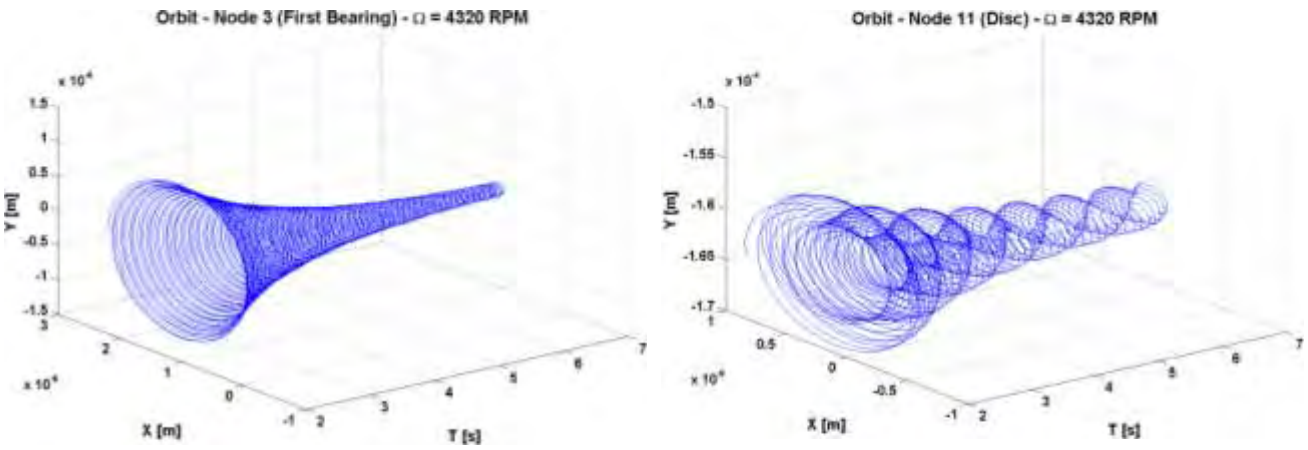

(a) (b)

Figure 3. Orbits at 4320 RPM for cylindrical bearing case: (a) First bearing's node; (b) Disc's node

However, when simulating a rotational speed after the instability threshold, the system presents a different behavior, as in Fig. 4. At the speed of 5220 RPM, the orbits amplitude increases over time, for both bearing and disc nodes, characterizing an unstable operation.

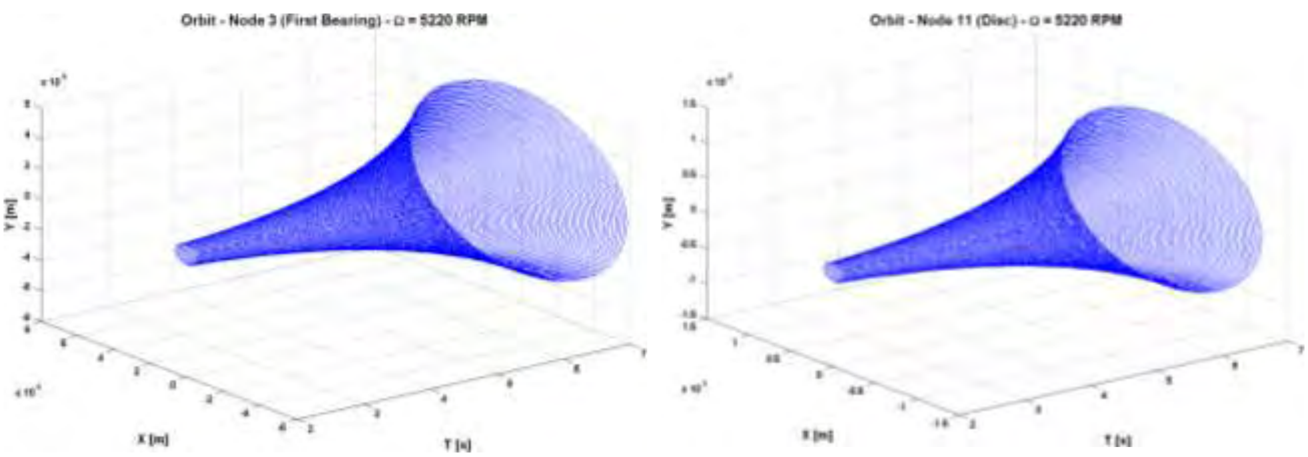

(a) (b)

Figure 4. Orbits at 5220 RPM for cylindrical bearing case: (a) First bearing's node; (b) Disc's node

Figure 5 presents the frequency response function (FRF) of the first bearing and disc nodes. The range of the rotational speeds is limited to a maximum of 7500 RPM, to help the graphic's visualization.

Figure 5(a) indicates the amplitudes for both X and Y directions, described by the shaft inside the bearing. It can be seen that the amplitude in the X direction is greater than in the Y direction, which is characteristic of a cylindrical bearings that have anisotropic coefficients. From the phase graphic, it can be seen that there is a variation of 180° (around 2400 RPM), indicating the critical speed of the mechanical system.

Figure 5(b) shows the same behavior regarding the natural frequency. However, the flexibility of the shaft overcomes the effects of anisotropy of the bearing, resulting in overlapping curves for the X and Y displacements.

ISSN 2176-5480

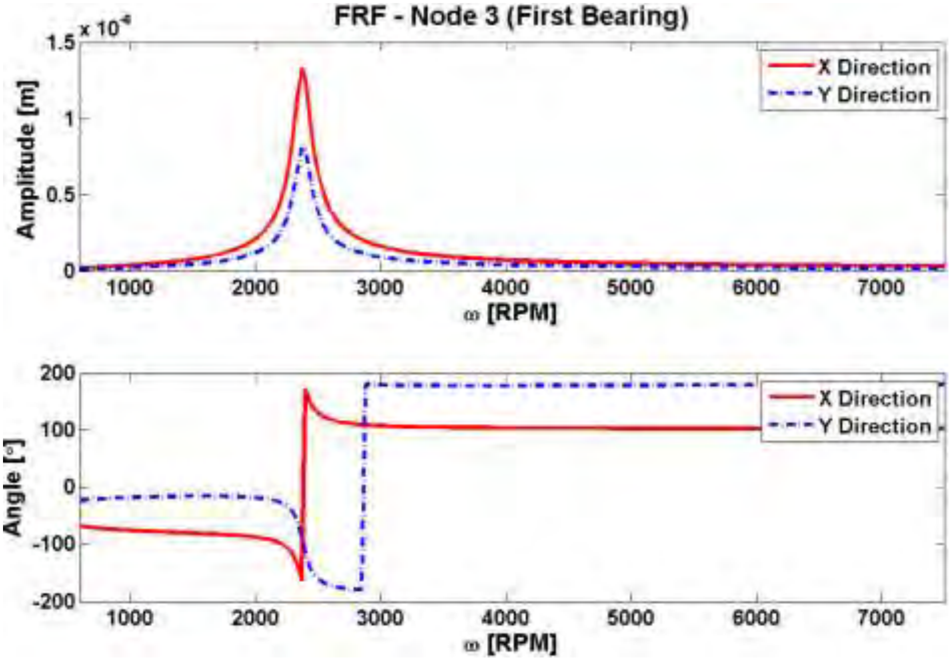

(a)

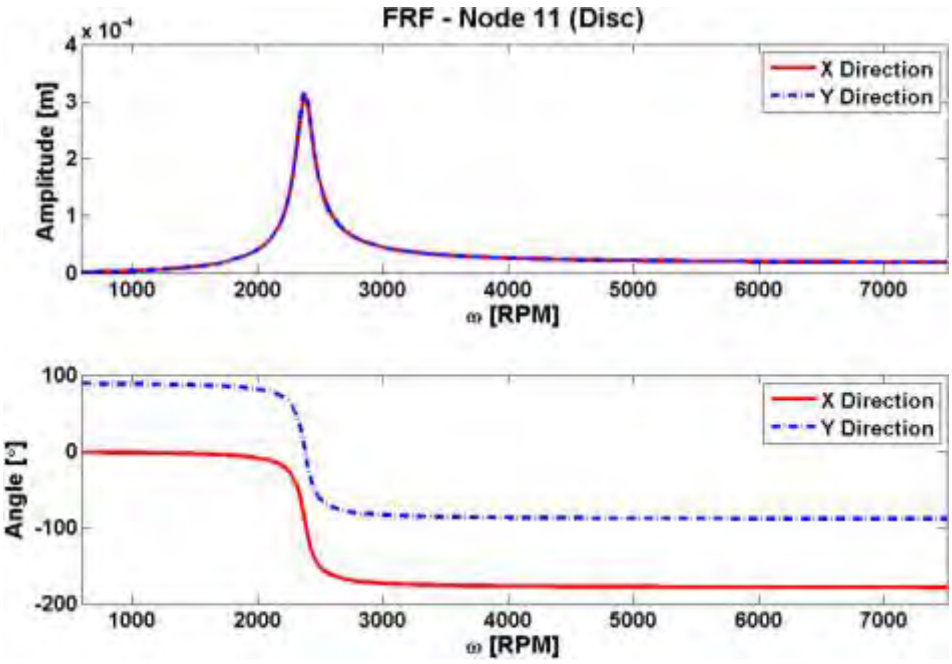

(b)
Figure 5. FRF for cylindrical bearing case: (a) First bearing's node; (b) Disc's node

The results obtained for the tilting-pad bearing are analogously analyzed. As done for the cylindrical bearing, initially the Campbell's diagram and damping ratio graphic are discussed. After that, the orbits at the rotational speeds of 4320 and 5220 RPM are obtained and finally the FRF is showed.

ISSN 2176-5480

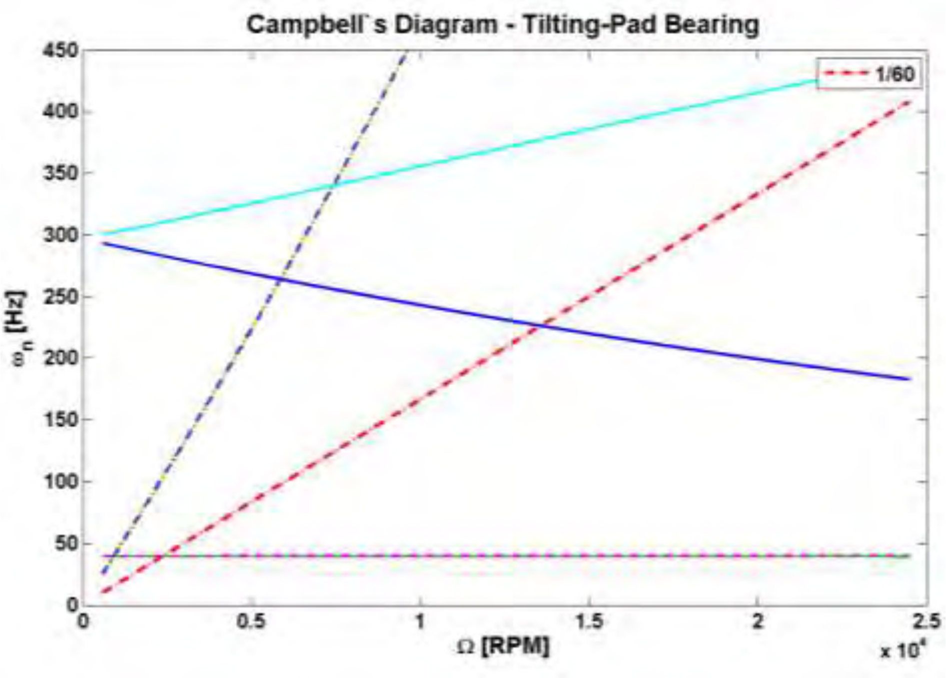

(a)

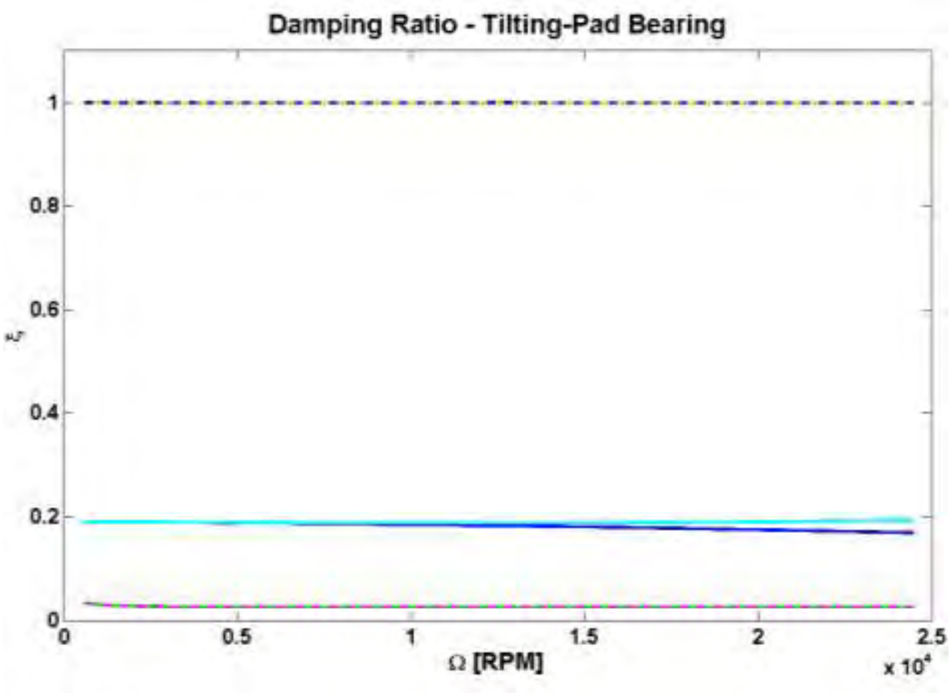

(b)

Figure 6. Free response for tilting-pad bearing case: (a) Campbell's diagram; (b) Damping ratio.

Figure 6 shows the shaft's natural frequencies curves, the bearings' frequencies curve and the rotational curve. When comparing Fig. 6(a) with the Campbell's diagram for the cylindrical bearing (Fig. 2), the curve of the bearings' frequencies is differently positioned due to the kind of bearing, with different frequencies' characteristics. The crossing points between the shaft's curves and the bearings' curves are also changed, which indicates that the rotational speed where instabilities occur with the use of cylindrical bearings is now stable.

The remaining curves presented the same behavior as viewed in Fig. 2(a). This is consistent, as those curves are related to the shafts' frequencies and present an indicative of the shaft's characteristics, not suffering significant influence of the bearings. Therefore, the first critical speed is still at 2400 RPM.

Figure 6(b) shows the damping ratio for the tilting-pad bearing case. As discussed before, the damping ratio value must be negative in order to be characterized as an unstable behavior. Analyzing the graphic on Fig. 6, values of negative damping ratio cannot be observed, indicating that the shaft is stable for the shaft's range of speed. This conclusion agrees with the analysis of the Campbell's diagram where no instability can be observed in the frequency range. Above all, no indication of instabilities at the rotational speed of 4800 RPM was found.

Nevertheless, Fig. 7 and 8 shows the orbits obtained in time domain, at the rotation speed of 4320 RPM (Figure 7) and 5220 RPM (Figure 8). Those orbits present a stable condition, not showing great variations in the displacements' amplitudes, as opposed as those found for the cylindrical bearing. From the analyses of the Campbell's diagram and damping ratio, it can be concluded that the Laval rotor supported by tilting-pad bearings does not present instabilities in the simulated frequency range.

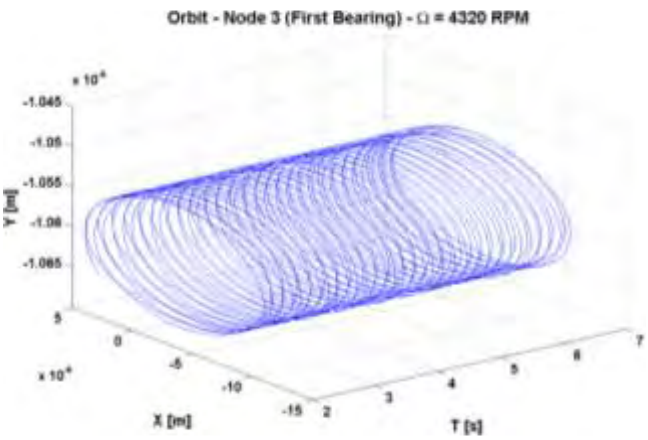

(a)

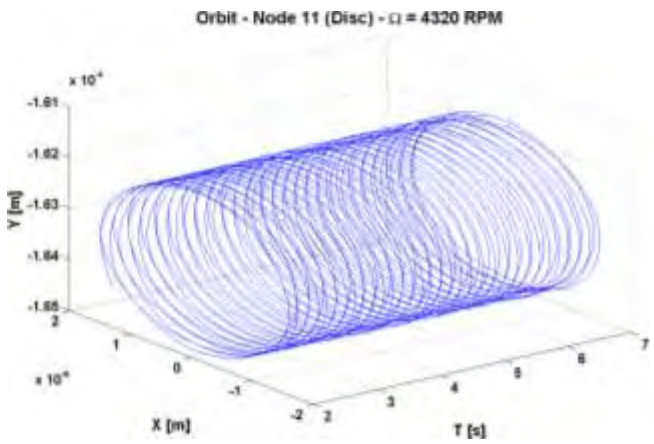

(b)

Figure 7. Orbits at 4320 RPM for tilting-pad bearing case: (a) First bearing's node; (b) Disc's node

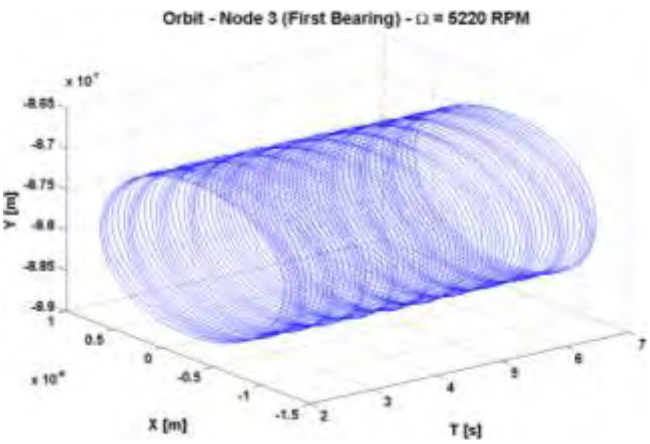

(a)

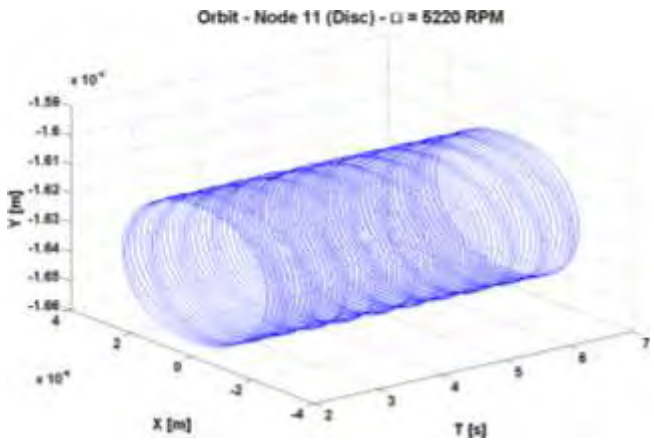

(b)

Figure 8. Orbits at 5220 RPM for tilting-pad bearing case: (a) First bearing's node; (b) Disc's node

At last, the FRFs for the tilting-tad bearing case are shown in Fig. 9. Figure 9(a) shows that the displacements X and Y are overlapped in the bearing node, so a circular trajectory can be expected, as opposed as the cylindrical case. This is characteristic of tilting-pad bearings that present direct coefficients approximately isotropic.

Both graphics on Fig. 9 present agreement regarding the critical velocity at 2400 RPM. This is a result that agrees with the previous analyses, as well. It can be observed that the graphic of Fig. 9(b), presents the same behavior as in Fig. 5(b), which means that the disc's amplitude is practically insensitive to the kind of bearing, because the shaft is more flexible than the bearings.

ISSN 2176-5480

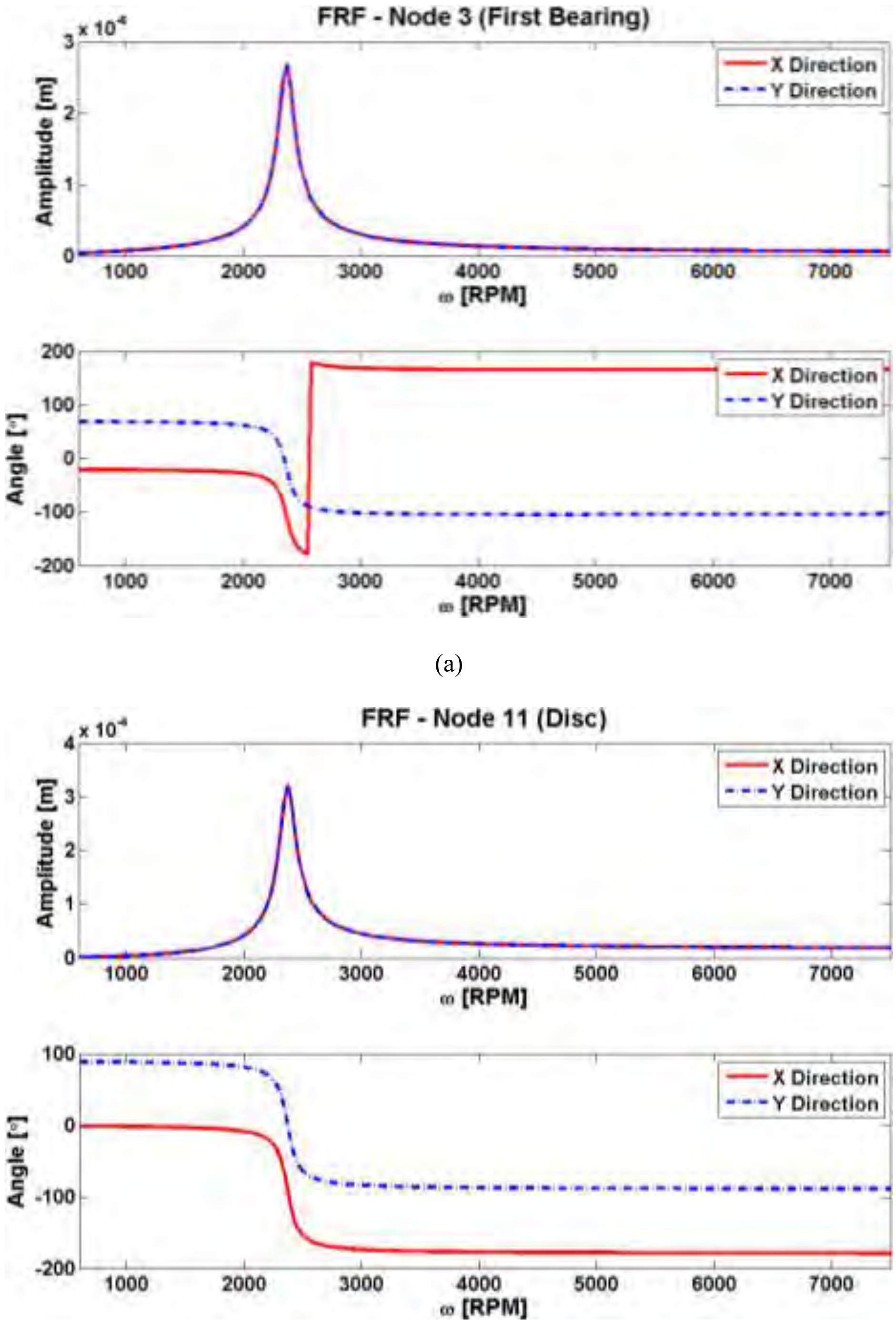

(a)

(b)

Figure 9. FRF for tilting-pad bearing case: (a) First bearing's node; (b) Disc's node

4. CONCLUSIONS

The analyses accomplished in this paper verify the differences on the rotor's dynamic behavior when it is supported by a cylindrical or a tilting-pad bearing. The cylindrical bearing presents an instable behavior on a specific rotational speed (about at double of the shaft's natural frequency), in which a negative value of the damping ratio was observed from the crossing points in the Campbell's diagram.

In other hand, the tilting-pad bearing did not present any kind of instabilities on the simulated frequency range. The Campbell's diagram showed a variation between the cylindrical and the tilting-pad bearings' frequencies, which is consistent with the difference between the kind of bearings and, consequently, their coefficients. The damping ratio did not present any negative values within the frequency range. Also, at the velocities where the cylindrical bearing had an instable operation, the tilting-pad showed a stable behavior.

5. ACKNOWLEDGEMENTS

The authors thank CNPq and FAPESP for the financial support of this research.

6. REFERENCES

Allaire, P., Parsell, J., Barret, L., *A Pad Perturbation Method for the Dynamic Coefficients of Tilting-Pad Journal Bearings.* Wear, 72, pp. 29-44, 1981.

Daniel, G. B., Cavalca, K. L. (orient.). *Desenvolvimento de um Modelo Termohidrodinâmico para Análise em Mancais Segmentados.* 2012. 236p. Dissertação (doutorado) - Universidade Estadual de Campinas, Faculdade de Engenharia Mecânica, Campinas, SP.

Hummel, C., *Kritische drehzahlen als folge der nachgiebigkeit des schmiermittels im lager*, Ph.D. Thesis, Eidgenössischen Technischen Hochschule in Zürich, 1926.

Lund, J. W., *Spring and damping coefficients for the tilting-pad journal bearing.* ASME Transactions, n.7, p.342-352, 1964.

Lund, J. W., *Evaluation of Stiffness and Damping Coefficients for Fluid Bearings.* The Shock and Vibration Digest, Vol. 11, No. 1, pp. 5–10, 1979.

Lund, J. W.,Pedersen, L. B., *The Influence of Pad Flexibility on the Dynamic Coefficients of a Tilting Pad Journal Bearing.* J. Tribol., 109(1):65-70, 1987.

Machado, T. H., Cavalca, K. L., 2009, *Evaluation of Dynamic Coefficients for Fluid Journal Bearings with Different Geometries*, In: 20th International Congress of Mechanical Engineering - COBEM 2009, Gramado-RS, Proceedings of the 20th International Congress of Mechanical Engineering. Rio de Janeiro : ABCM - Associação Brasileira de Ciências Mecânicas, v. 1. p. 1-11.

Mendes, R. U., Cavalca, K. L. (orient.), *Desenvolvimento de um Sistema de Atuação Magnética para Excitação de Sistemas Rotativos.* 2011. 140p. Dissertação (mestrado) - Universidade Estadual de Campinas, Faculdade de Engenharia Mecânica, Campinas, SP.

Nelson, H. D., *A finite rotating shaft element using Timoshenko beam theory.* ASME Journal of Mechanical Design, v. 102, n. 4, p. 793-803, 1980.

Nelson, H. D.; McVaugh, J. M., *The Dynamics of Rotor-Bearing Systems Using Finite Elements.* Journal of Engineering for Industry, p.593-600, May 1976.

Newkirk, B. L., and Taylor, H. D, *Shaft Whipping due to Oil Action in Journal Bearings,* General Electric Review, Vol. 28, n. 8, 1925, pp. 559-568.

Ocvirk, F., 1952, *Short Bearing Approximation for Full Journal Bearing*, NACA TN 20808.

Pinkus, O., 1956, *Analysis of Elliptical Bearings*, Trans. ASME, v. 78, pp. 965-973.

Pinkus, O., 1958, *Solution of Reynolds Equation for Finite Journal Bearings*, Trans. ASME, v. 80, pp. 858-864.

Pinkus, O., 1959, *Analysis and Characteristics of Three-lobe Bearings*, Journal of Basic Engineering, pp. 49-55.

Reynolds, O., *On the Theory of Lubrication and Its Application to Mr. Beauchamp Tower's Experiments Including an Experimental Determination of the Viscosity of Olive Oil.* Philos. Trans. R. Soc. London, Series A, Vol. 177, Part 1, 1886, pp.157-234.

Sommerfeld, A., *Zur Hydrodynamischen Theorie der Schmiermittelreibung.* Zs. Math. and Phys., Vol. 50, No.1, 1904, pp.97-155.

Stodola, A., *Kritische Wellenstörung infolge der Nachgiebigkeit des Oelpolsters im Lager*, Schweizerische Bauzeitung, Vol. 85/86, pp. 265-266, 1925.

Tuckmantel, F. W., Cavalca, K. L. (orient.)., *Integração de sistemas rotor-mancais hidrodinâmicos-estrutura de suporte para resolução numérica.* 2010. 159 p. Dissertação (mestrado) - Universidade Estadual de Campinas, Faculdade de Engenharia Mecânica, Campinas, SP.

7. RESPONSIBILITY NOTICE

The authors are the only responsible for the printed material included in this paper.